Asymmetric Fabry-Pérot interferometric cavity for fiber optical sensors

Shaoji Jiang (江绍基), Youcheng Liang (梁有程), Xi Zhu (朱 析), and Hezhou Wang (汪河洲)

State Key Laboratory of Optoelectronic Materials and Technologies, Sun Yat-Sen University, Guangzhou 510275

Received April 3, 2006

Good linearity and wide dynamic range are the advantages of asymmetric Fabry-Pérot (F-P) interferometric cavity, whose realization has been long for. Based on optical thin film characteristic matrix theory, an asymmetric F-P interferometric cavity with good linearity and wide dynamic range is designed. And by choosing the material of two different thin metallic layers, the asymmetric F-P interferometric cavity is successfully fabricated. The design theory and method of this asymmetric F-P interferometric cavity have been described in detailed. In this paper an asymmetric F-P interferometric cavity used in fiber optical sensor is reported.

OCIS codes: 060.2370, 050.2230.

Fiber optical sensors have been applied in various measurements because of their inherent advantages[1]. Fabry-Pérot (F-P) interferometric sensors possess good sensitivity and resolution. Therefore, fiber optical F-P interferometric sensors have been used in the measurement of various physical parameters, such as temperature[2,3], strain[4,5], vibration[6], displacement[7], and pressure[8,9]. The basic F-P interferometer incorporates an in-line or internal reflector formed by the interface between bond or fusion spliced fiber, the end face of the fiber typically having been precoated with a reflective dielectric layer such as titanium. It is well known, the linearity of sine function is not good and its range of linearity is very narrow, due to around the maximum and the minimum, the responses are much slower than that far from the extrema. These limit the measurement range and sensitivity of the F-P interferometic fiber optical sensors. To design an F-P cavity optical sensor with good linearity and wide dynamic range is long for. The asymmetric F-P interferometer cavity is put forward in this paper.

The asymmetric F-P interferometric cavity, which consists of a dielectric tunable layer (usually air) between a high reflector considered as ideal metal and a partial reflector consisting of two thin metallic films, is shown in Fig. 1. When the dielectric tunable layer of the F-P interferometer is very thin, this system can be considered as a multiple-layer thin film system and can be analyzed with optical thin film theory. Here, the single-mode fiber (SMF) is considered as incident medium and the metallic high reflector as substrate; a multiple-layer thin film consists of the middle dielectric layer and multiple thin metallic films is deposited on the end face of the SMF. The sensing mechanism is provided by the changes of phase thickness in the reflected or transmitted interferogram that are due to changes in the optical path length of the resonant cavity under external sensing parameters such as pressure, temperature, strain and so on. The response of the sensors can be obtained if the relationship between the reflectance and the parameter of the dielectric layer is known. In practical application, the parameter modulated is usually the phase thickness of dielectric layer, so the relationship between the reflectance and the phase thickness of the dielectric layer is investigated in this paper. The thin film system can be expressed as[10] $G\,|M_1M_2L|\,M_g$, G denotes the incident media, its refractive index is written as n_0. M_1, M_2 denote the metallic thin films deposited on the end face of the SMF; their complex refractive indices are written as N_1, N_2, and their thicknesses are written as d_1, d_2. M_g denotes the substrate with the complex refractive index N_g. L denotes the dielectric tunable layer with the refractive n_m and the thickness d_m.

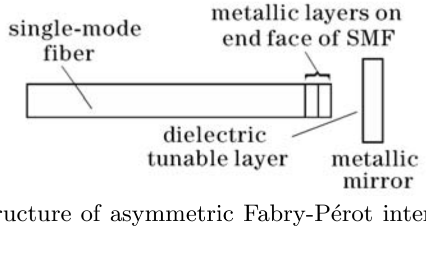

Fig. 1. Structure of asymmetric Fabry-Pérot interferometric cavity.

When the light is normal incidence, the interference matrix of the assembly can be written as[11]

$$\begin{bmatrix} B \\ C \end{bmatrix} = \left(\prod_{r=1}^{k} \begin{bmatrix} \cos\delta_r & j\sin\delta_r/N_r \\ jN_r\sin\delta_r & \cos\delta_r \end{bmatrix} \right) \times \begin{bmatrix} \cos\delta_m & j\sin\delta_m/n_m \\ jn_m\sin\delta_m & \cos\delta_m \end{bmatrix} \cdot \begin{bmatrix} 1 \\ N_g \end{bmatrix}. \quad (1)$$

And the reflectance R of the assembly can be given as

$$R = \left| \frac{n_0 - \frac{C}{B}}{n_0 + \frac{C}{B}} \right|^2 , \quad (2)$$

where $N_r = n_r - jk_r$, $\delta_r = 2\pi N_r d_r/\lambda$, $Ng = n_g - jk_g$, $\delta_m = 2\pi N_m d_m/\lambda$, δ denotes the phase thickness.

We have found that the $R-\delta_m$ response can approximate to a saw wave function and the sensing result can be satisfied, when the films on the end face of SMF are two different thin metallic layers described as following and their parameters are fitted. The first layer is the metal whose n as real part of the complex refractive index is closed to k as imaginary part, such as Cr, Ni and so on. The second layer is the metal whose n is much less than k, such as Au, Ag, Al, Cu and so on.

If the metallic film is thin adequately, d_1, $d_2 \ll \lambda$, then

$$\delta_i = 2\pi(n_i - jk_i)d_i/\lambda \approx 0, \quad (i = 1, 2). \tag{3}$$

So the characteristic matrix of the two metal films A_1, A_2 can be simplified as

$$A_1 = \begin{bmatrix} 1 & j2\pi d_1/\lambda \\ 4\pi k_1^2 d_1/\lambda & 1 \end{bmatrix}, \tag{4}$$

$$A_2 = \begin{bmatrix} 1 & j2\pi d_2/\lambda \\ -j2\pi k_2^2 d_2/\lambda & 1 \end{bmatrix}. \tag{5}$$

Then

$$A_1 A_2 = \begin{bmatrix} 1 + 4\pi^2 k_2^2 d_1 d_2/\lambda^2 & j2\pi(d_1 + d_2)/\lambda \\ 2\pi(2k_1^2 d_1 - jk_2^2 d_2)/\lambda & 1 + j8\pi^2 k_1^2 d_1 d_2/\lambda^2 \end{bmatrix}. \tag{6}$$

It can be simplified as

$$A_1 A_2 = \begin{bmatrix} 1 & j2\pi(d_1 + d_2)/\lambda \\ 2\pi(2k_1^2 d_1 - jk_2^2 d_2)/\lambda & 1 \end{bmatrix}. \tag{7}$$

The characteristic matrix of assembly, by analogy with Eq. (1) is written as

$$\begin{bmatrix} B \\ C \end{bmatrix} = \begin{bmatrix} c_1 - c_2(F_1/k_1 + F_2/k_2) \\ c_1(2k_1F_1 - jk_2F_2) + jc_2 \end{bmatrix}, \tag{8}$$

where $c_1 = \cos\delta_m + \frac{k_g \sin\delta_m}{n_m}$, $c_2 = n_m \sin\delta_m - k_g \cos\delta_m$, $F_i = 2\pi k_i d_i/\lambda$, $(i = 1, 2)$. The reflectance is given as

$$R = 1 - \frac{8n_0 k_1 F_1 c_1 \left[c_1 - (F_1/k_1 + F_2/k_2)\, c_2\right]}{\left\{n_0 \left[c_1 - (F_1/k_1 + F_2/k_2) c_2)\right] + 2k_1 F_1 c_1\right\}^2 + (k_2 F_2 c_1 - c_2)^2}. \tag{9}$$

Equation (9) can be simplified as

$$R = 1 - \frac{8n_0 k_1 F_1}{(n_0 + 2k_1 F_1)^2 + (k_2 F_2 - c_2/c_1)^2}. \tag{10}$$

The derivative of reflectance referenced to δ_m is

$$R' = \frac{16 n_0 n_m k_1 F_1 \left[k_2 F_2 + n_m \frac{\sin(\delta_m + \delta_{01})}{\sin(-\delta_m + \delta_{02})}\right] \left[\frac{\sin(\delta_{02} - \delta_{01})}{\sin^2(-\delta_m + \delta_{02})}\right]}{\left\{(n_0 + 2k_1 F_1)^2 + \left[k_2 F_2 + n_m \frac{\sin(\delta_m + \delta_{01})}{\sin(-\delta_m + \delta_{02})}\right]^2\right\}^2}, \tag{11}$$

where $\delta_{01} = \arctan(n_m/k_g)$, $\delta_{02} = \arctan(k_g/n_m)$.

The position of the extrema is determined by following conditions: when $\delta_m = \delta_{02} + k\pi$, R is maximum, and $R = 1$. When $\delta_m = -\delta_{01} + \arctan\frac{k_2 F_2 \sin(\delta_{01} + \delta_{02})}{-n_m + k_2 F_2 \cos(\delta_{01} + \delta_{02})} + k\pi$, R is minimum, and $R = 1 - \frac{8n_0 k_1 F_1}{(n_0 + 2k_1 F_1)^2}$.

From Eq. (11), it is obvious that the $R - \delta_m$ curve is the periodic function with a period of π, while R varies between 1 and 0 with a maximum and a minimum in one period. The minimum of R is determined by the parameters of first metallic layer. For sensing application, a high interference contrast is wanted. The highest contrast can be obtained by adjusting the thickness of the first metallic layer to get $n_0 = 2k_1 F_1$ and $R = 0$. And the measurement range of the sensor can be improved by enlarging the monotony interval of the $R - \delta_m$ response. In a period, the ascending interval can be compressed, at the same time the descending interval is enlarged inversely by changing the position of the extremum. The position of the maximum, which is determined by the material parameters of the metallic high reflector and the dielectric tunable layer of the interferometric cavity, has a small adjustable range. The position of the minimum, which is determined by the parameters of the high reflector, tunable layer and the second metallic layer on the end face of fiber, can be shifted markedly by adjusting the parameter of second metallic layer (especially the real part of the complex refractive index n_1 and the imaginary part of the complex refractive index k_1). Figure 2 shows the calculated $R - \delta_m$ response of the interferometric cavity at different values of n_2 and k_2. From Fig. 2, we can find that when $n_2 \ll k_2$, the descending interval of the $R - \delta_m$ curve is enlarged, the position of minimum is very close to the position of the maximum and descending interval

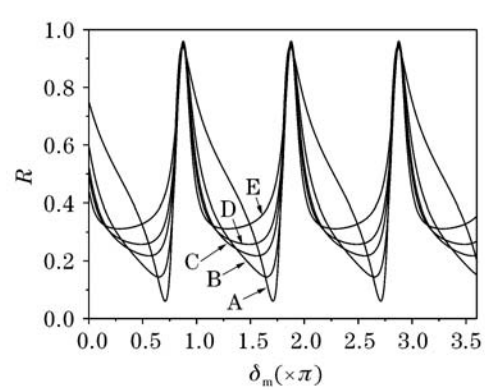

Fig. 2. Calculated $R - \delta_m$ response of the interferometric cavity, for which $N_1 = 3.45 - 3.45j$; $N_2 = 0.2 - 4.6j$ (A), $1.4 - 4.6j$ (B), $2.6 - 4.6j$ (C), $3.8 - 4.6j$ (D), $4.6 - 4.6j$ (E); $d_1 = 6$ nm and $d_2 = 13$ nm.

is close to π. Simultaneity, the linearity of the response is improved in the monotony interval.

According to above-mentioned theory, an asymmetric F-P interferometer, which consists of fiber, Cr, Cu, air, Cu, is designed for instance. The parameters are described as follows: the wavelength is 850 nm, n_0 of fiber is 1.45, N_1 of the first metallic layer Cr is $3.45 - 3.45j$, N_2 of the second metallic layer Cu is $0.17 - 4.84j$, and the thickness of Cr thin film is 6 nm, the thickness of Cu thin film next to Cr is 13 nm. Using the interference matrix method and the expression deduced in this paper, we have calculated the $R - \delta_m$ response of the interferometer cavity, as shown in Fig. 3.

The interferometer cavity with good linearity and wide dynamic range was fabricated by depositing the multi-layer thin films on a fused silica substrate with the formula on a fused silica substrate with the formula $G\,|M_1M_2L|\,M_g$ by electron beam deposition, where $M_1 = 6$ nm, $M_2 = 13$ nm, $M_g = 200$ nm, and the thickness of L varied from 350 to 1000 nm. But in the experiment, the dielectric tunable layer L had been instead of with SiO_2 ($n_m = 1.45$). By depositing the multi-layer thin films with different tunable layers, we have fabricated the interferometer cavity with different thicknesses of tunable layer. The reflectivity of the interferometer cavity at the wavelength of 850 nm was measured by Lambda 900 spectrophotometer. By transforming the thickness of the tunable layer into phase thickness, we have obtained the reflectance of the interferometric cavity at different phase thicknesses, as shown in Fig. 4.

Figure 4 shows good agreement with the theoretical values, but near their maximum positions, the descending interval is narrower than that of theoretical expectation; this may be caused by the monitoring errors of the optical thickness and the calculating errors of the material parameters. The reflectance maximum calculated or measured is a little less than 1, because the real part of the complex refractive of the high reflector is not completely zero and thus its reflectance is less than 100%. From Figs. 3 and 4, we can see that the interferometer structure designed with above method can have a satisfying response. The minimum of the response is closed to zero; and the maximum is closed to 97%. Different from traditional F-P interferometer, the reflectance has evident variety near all extrema, and the linearity of the descending and ascending interval has been enhanced. Therefore, it is of advantage to increase the sensitivity of the measurement. In this instance, the monotony ascending interval has been compressed. At the same time, the monotony descending interval is close to π, so the dynamic range of the interferometric cavity can be enlarged evidently.

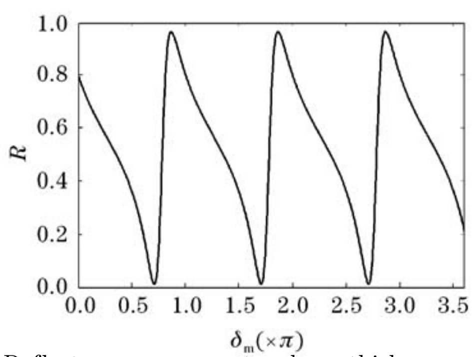

Fig. 3. Reflectance response to phase thickness calculated with Eq. (10).

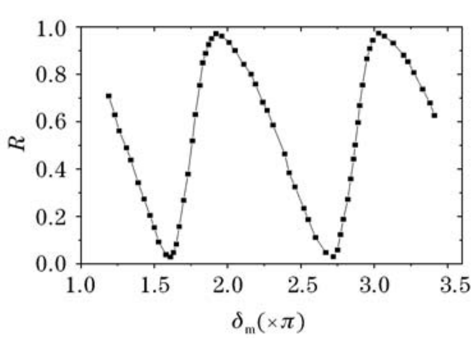

Fig. 4. Results of reflectance response to phase thickness.

A novel asymmetric F-P interferometer structure used in fiber optical sensors is reported in this paper. This F-P interferometer structure consists of a tunable layer between a high reflector and a partial reflector to form a multiple-layer thin film system, in which the important point is that the high reflector is Cu, and partial reflector consisting of two thin metallic films, one is Cu, and the other is Cr. In this paper the process of calculation with interference matrix method has been described. Furthermore, this asymmetric F-P interferometer structure has been fabricated and the experimental results demonstrate that this structure can work efficiently in measurement for weak signal.

This work was supported by the National "863" Project of China (No. 2003AA311022), the National "973" Project of China (No. 2004CB719804), the National Natural Science Foundation of China (No. 10274108), and the Natural Science Foundation of Guangdong Province of China. H. Wang is the author to whom the correspondence should be addressed, his e-mail address is stswhz@zsu.edu.cn.

References

1. A. D. Kersey and A. Dandridge, IEEE Trans. Comp. Hybrids Manuf. Technol. **13,** 137 (1990).
2. G. Cocorullo, F. G. Della Corte, M. Iodice, I. Rendina, and P. M. Sarro, Sensors and Actuators A **61,** 267 (1997).
3. L. C. Gunderson, Proc. SPIE **1267,** 194 (1990).
4. E. J. Friebele, M. A. Putam, A. D. Kersey, A. S. Greenblatt, G. P. Ruthven, M. H. Krim, and K. S. Gottschalck, Proc. SPIE **3042,** 100 (1997).
5. I.-B. Kwon, M.-Y. Choi, and H. Moon, Sensors and Actuators A **112,** 10 (2004).
6. T. Y. Liu, M. Berwick, and D. A. Jackson, Rev. Sci. Instrum. **63,** 2164 (1992).
7. C. Zhang and X. Wang, Chin. Opt. Lett. **1,** 459 (2003).
8. M. J. Gander, W. N. MacPherson, J. S. Barton, R. L. Reuben, J. D. C. Jones, R. Stevens, K. S. Chana, S. J. Anderson, and T. V. Jones, IEEE Sensors Journal **3,** 102 (2003).
9. H. Xiao, J. Deng, Z. Wang, W. Huo, P. Zhang, M. Luo, G. R. Pickrell, R. G. May, and A. Wang, Opt. Eng. **44,** 054403 (2005).
10. Y. Kim and D. P. Neikirk, Sensors and Actuators A **50,** 141 (1995).
11. H. A. Macleod, *Thin-Film Optical Filters* (2nd ed.) (Adam Hilger, Bristol, UK, 1986) Chap.2, p.43.